Multiple-Shift Code Acquisition of Optical Orthogonal Codes in Optical CDMA Systems

Abtin Keshavarzian, *Student Member, IEEE,* and Jawad A. Salehi, *Member, IEEE*

***Abstract*—In this paper, we introduce a new and advanced algorithm, namely, multiple-shift algorithm for code acquisition in optical code-division multiple access (CDMA) systems using unipolar optical orthogonal codes (OOCs) as signature sequences. We analyze the performance of the newly proposed algorithm and obtain a bound on its performance and show its advantage in reducing the mean time of synchronization when compared with other synchronization methods. The algorithm can be used with many different receiver structures, like active or passive correlator with or without hardlimiter(s). However, in this paper, we only consider the simple active correlator structure for further discussions and analysis.**

***Index Terms*—Code acquisition and synchronization, code-division multiple access (CDMA), optical CDMA, optical orthogonal codes (OOCs).**

I. Introduction

OPTICAL synchronization will undoubtedly play a central role in helping to introduce all-optical code-division multiple access (CDMA) networks for future bursty and packet-based communications systems. As the speed of all-optical packet communications increases unboundedly, the success of optical synchronization will rest upon introducing a very efficient algorithm in order to obtain the synchronization with minimal required time. The majority of published works on all-optical CDMA systems [1]–[5] assumes perfect synchronization between each receiver and transmitter pair. However, Yang [10] considered a simple synchronization method for noncoherent optical CDMA and highlighted the importance of synchronization by showing the degradation in the performance of the system when the synchronization between receiver and transmitter is not ideal. Later, Mustapha and Ormonroyd introduced, first, a serial-search synchronizer [11] and second, a dual-threshold sequential method [12] for synchronization of an optical orthogonal code (OOC)-CDMA system.

In [6], the authors considered the performance of simple serial-search algorithm for code acquisition in an optical CDMA system using OOCs. It was shown that the mean time required for synchronization is in the order of half code length bits duration. Long code lengths may be used in a typical system which, therefore, requires a long period for synchronization. In this paper, we introduce and analyze a new and advanced algorithm, namely, multiple-shift algorithm, which not only is simple in its structure but also greatly improves the performance of synchronization process. With the help of Markov chain model, we analyze the performance of the proposed algorithm. We will obtain a bound, regardless of the OOC optical receiver structure used [4], on the performance of the proposed algorithm and show its advantage in reducing the mean time of synchronization when compared with the simple serial-search algorithm. Although this algorithm can be used with many different receiver structures like active or passive correlator and with or without hardlimiter(s) [2]–[4], we only consider the simple active correlator structure for further discussion and analysis. To this end, some approximate results for the active correlator receiver structure are obtained, then compared with the result obtained from simulation to show their accuracy

The rest of this paper is organized as follows. In Section II, the system model and the multiple-shift algorithm are described. In Section III, we use Markov chain model, to evaluate the performance of the proposed algorithm by computing the mean acquisition time in terms of probabilities of false alarm and detection. Subsequently we use the obtained results to acquire a general bound on the performance of the multiple-shift algorithm. In Section IV, expressions for the probabilities of false alarm and detection are obtained. In Section V, some numerical results are illustrated and some thoughts on the use of the system are discussed. Section VI concludes this paper and discusses on other uses of the multiple-shift algorithm.

II. System Model

In this section we describe the system model. Fig. 1 shows the general conceptual structure of an OOC-CDMA network [1]–[5]. There are N users in the network each with a transmitter–receiver pair that want to send data through the only available channel (*e.g.,* a fiber-optic link), so they need to share the channel using a multiaccess technique. An OOC [1]–[3] is given to each user (transmitter–receiver pair) to allow them to form CDMA system. At the transmitter side after modulating and encoding the signals from different users, they are all added together and sent through the channel to the other side, where a copy of the sum signal is received by all users. Each receiver will then decode the data that is sent from its own transmitter pair. Therefore, in Fig. 1, the channel is shown as a $N \times N$ star coupler. The received signal $r(t)$ is given by

$$r(t) = \sum_{n=1}^{N} s_n (t - \tau_n) \tag{1}$$

Paper approved by I. Andonovic, the Editor for Optical Networks and Devices of the IEEE Communications Society. Manuscript received December 8, 2001; revised January 11, 2002. This work has been done as part of Contract 7931410 with Iran Telecommunication Research Center (ITRC), Tehran, Iran.

A. Keshavarzian is with the Electrical Engineering Department, Stanford University, Stanford, CA 94305 USA (e-mail: abtink@stanford.edu).

J. A. Salehi is with the Electrical Engineering Department, Sharif University of Technology, Tehran, Iran.

Digital Object Identifier 10.1109/TCOMM.2005.843456

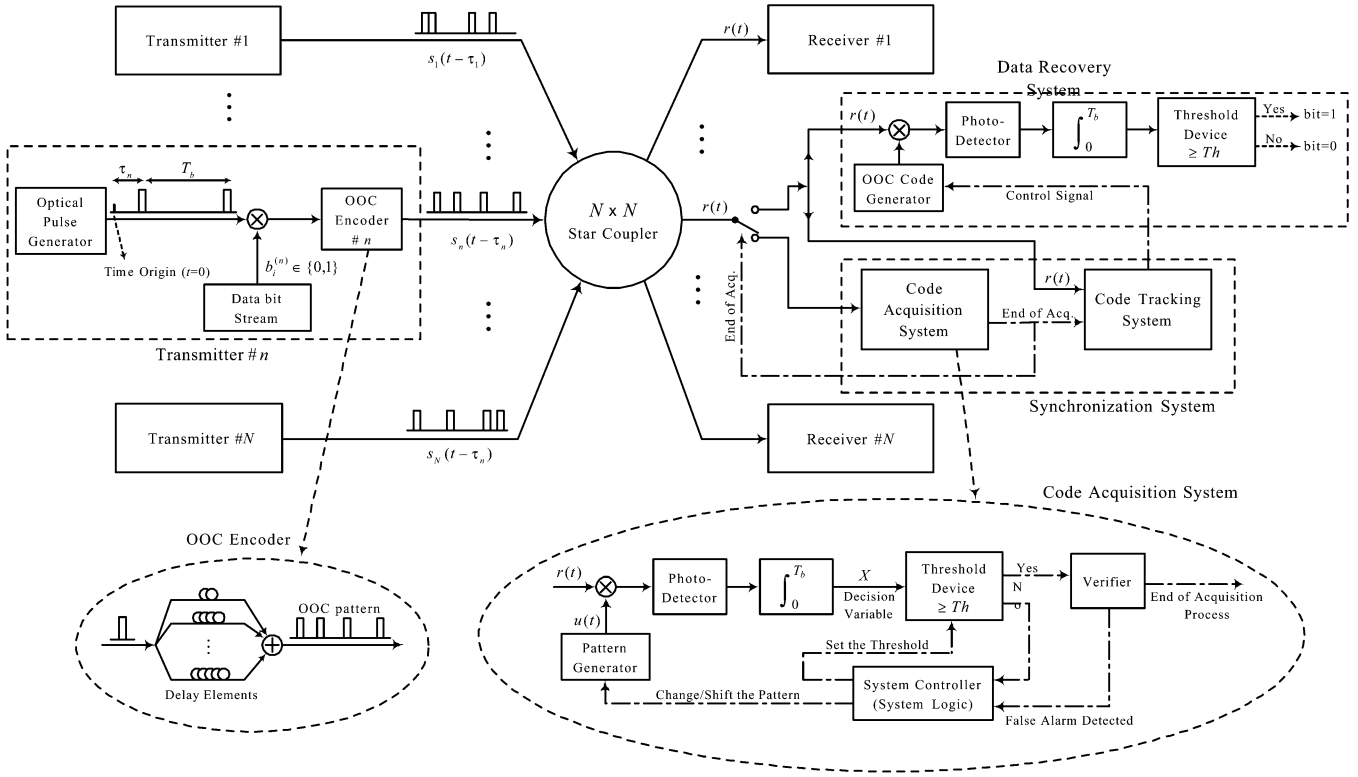

Fig. 1. A typical OOC-CDMA network.

where $s_n(t)$ is the signal of nth user and $\tau_n \in [0, T_b)$ denotes the time offset of nth user's signal from a selected time origin. The modulation used is on-off-keying (OOK), i.e., for a bit "one", the sender transmits a pulse and for a "zero" bit nothing is sent. The bit rate is assumed to be the same for all users and T_b denotes one bit time duration. Thus, $s_n(t)$ can be expressed as

$$s_n(t) = \sum_{i=-\infty}^{\infty} b_i^{(n)} c_n(t - iT_b) \tag{2}$$

where $b_i^{(n)}$ shows the ith bit of nth user $\left(b_i^{(n)} \in \{0, 1\}\right)$, and $c_n(t)$ is OOC code of nth user.

An OOC code is a binary sequence of length F and weight K of the form $(a_0, a_1, \ldots, a_{F-1})$ (with each $a_j \in \{0, 1\}$ and $\sum_{j=0}^{F-1} a_j = K$) which has bounded auto-correlation. The cross-correlation between two different OOC codes should also be bounded. We assume that OOCs with autocorrelation and cross-correlation values bounded by one, are used in the network as in [1], [2]. Hence if $\left(a_0^{(n)}, a_1^{(n)}, \ldots, a_{F-1}^{(n)}\right)$ denotes the OOC code of nth user, the $c_n(t)$ can be written as

$$c_n(t) = \sum_{j=0}^{F-1} a_j^{(n)} P_{T_c}(t - jT_c) \tag{3}$$

where T_c which is called *chip* duration, is $1/F$ of one bit duration, *i.e.,* $T_b = FT_c$, and $P_{T_c}(t)$ is a rectangular pulse of length T_c defined as follows

$$P_{T_c}(t) = \begin{cases} 1, & 0 \le t < T_c \\ 0, & \text{otherwise.} \end{cases} \tag{4}$$

In Fig. 1, a typical transmitter structure is also shown. An optical pulse generator, generates a pulse train with width T_c at rate $1/T_b$. These pulses are modulated by the data bits using a simple on-off switch (shown as a multiplier in the figure), then the signal passes through an OOC encoder, which using some delay elements, converts a single pulse into an OOC pattern.

At the receiver side, the data recovery system, shown in Fig. 1, is one of the possible structures which is called the active correlator structure (see [4] for more details about different receiver structures). For this structure, the received signal is multiplied with a replica of the OOC code (generated by a local OOC code generator), and photo-detected and then its integral is computed over one bit period to form a decision variable. This decision variable is in fact a measure of correlation between the received signal and the locally generated OOC code. It is then compared with a threshold. If the correlation is high (the decision variable is larger than the threshold), the receiver decodes the transmitted bit as a "one", otherwise it is decoded as a "zero". If the locally generated code used in the data recovery system is not aligned with the code pattern in the received signal, no decoding is possible. Hence, in order to decode the transmitted bits correctly, the receiver is required to know both the OOC code, and the value of τ_n to generate a correct shift of the code. It is the task of the "*synchronization system*" to estimate the value of τ_n or equivalently find the correct shift of the code.

A. Synchronization

The synchronization is typically done in two steps. First the uncertainty region of τ_n is partitioned into small fragments of length T_c (or a fraction of T_c) and a search is performed to find the fragment which contains the correct value. Then in second

step, the exact value of τ_n is estimated within this fragment. The first step is called "*code acquisition*" or "*coarse synchronization*" and it is a search problem (or a multiple-hypothesis testing problem). The second step, which is generally performed by some feedback tracking loops, is called "*fine synchronization*" or "*code tracking*".

Each receiver first starts the code acquisition process until it finds an acceptable estimate of τ_n, then data recovery can start while at the same time the tracking system is continuously running and updating the value of τ_n to ensure that the correct shift of the code is used in the decoding process.

The uncertainty region for τ_n is $[0, T_b)$. It is divided into F fragments (which are also called *cells*), each having a duration of T_c. Then the system searches these F possible cells to find the one within which the actual value of τ_n is located.

To check each cell, a simple correlation test is adopted as shown in Fig. 1. The test is similar to the decoding method described before. We assume that the transmitter continuously sends bit one during the whole code acquisition process [1]. The received signal is correlated with a shifted version of the desired user's OOC code which corresponds to the cell being examined. If the output of the correlator exceeds a predefined threshold the cell is accepted as the correct cell, otherwise the cell is rejected. The time required to check the state of correctness or incorrectness of each cell is called "*dwell time*" in literature [7]–[9]. To be able to get all the K pulses of an OOC code, the the dwell time of the system must be at least one bit time or multiples of it to cover the whole code length. We select dwell time to be one bit duration. Hence, to check each cell, we spend one bit time (T_b), and later we will talk about the number of bits required for the code acquisition process.

Once the synchronization process is described as a search problem, the strategy that the synchronization system should employ to perform this search must be selected. One method is the popular technique of simple serial-search, *i.e.,* the search starts from a randomly selected (or pre-specified) cell (or shift) and then the system serially examines the other shifts in a pre-specified order until the correct shift is found. In [6] the performance of such algorithm is analyzed for an OOC-CDMA system. It is shown that approximately the code acquisition requires $F/2$ (half code length) bits to find the correct shift. In this paper, we describe and analyze a more advanced and more efficient algorithm, called "multiple-shift algorithm" which performs the code acquisition process exceedingly faster than the simple serial-search algorithm.

B. Multiple-Shift Algorithm

The multiple-shift algorithm has an initializing part and two modes. Initially the F different shifts (or cells) in the search space are partitioned into Q equal-sized groups each containing M different shifts. M is a parameter of the algorithm and later we will discuss about how to select its value. Q is related to M by

$$Q = \left\lfloor \frac{F}{M} \right\rfloor. \tag{5}$$

Note that when M is not a divisor of F, Q is the upper closest integer to the ratio (F/M) which implies that one of the groups will have fewer elements than others.

The algorithm has two modes. In the first mode it examines the cells in a group all at the same time. In this way it is possible that the algorithm rejects a group of cells with just one test. If the test does not reject the group the second mode begins and each element in the group is examined individually.

To examine a group of cells (shifts), a correlation test is again used. Instead of correlating the received signal with only one single shift, we compute its correlation with the sum of M different shifts of the code to get the decision variable. Since the structure is linear with respect to the locally generated code pattern, the output computed in this way will be the linear combination of the output of the correlator due to each shift. If the computed decision variable does not exceed a pre-determined threshold level, all the M shifts in that group are rejected and then another group is considered to be examined.

When the decision variable exceeds the threshold, it indicates that one of the M shifts may be the correct shift, so to find it the algorithm switches to second mode. In second mode each of the M shifts are examined separately, i.e., the first shift in the group is examined and if rejected, the next shift is considered an so on, until all the M shifts in that group are examined. When all the M shifts are taken into account exclusively and rejected, the algorithm switches back to first mode and continues the search with the next group. Note that the thresholds used in the two modes can be different.

Multiaccess interference and other noise sources may cause error in deciding about the correctness of a shift in second mode or a group in the first mode. Such error is called "*false alarm*". A false alarm occurs in the first mode when none of the M shifts are correct but the decision variable exceeds the threshold, while in the second mode we get a false alarm when the shift is not correct but the correlator's output indicates differently.

It is the task of verification mode to detect false alarms in the second mode. Verification system initiates when it is claimed that the correct shift is found. We assume that the verification system, after spending some time which is called "*penalty time*", will detect false alarm. In fact for analyzing the performance of the code acquisition system, one does not need to know the structure or algorithm used during the verification process, as long as the penalty time is known [7], [8].

Another error that may occur in the search process is the missing of the correct shift position. Like false alarm, this error may arise in both modes of the algorithm. However, since the interference in the OOC-CDMA system can only increase the output, with the proper selection of the thresholds, the probability of missing the correct shift can be made very small, or equivalently the probability of detecting the correct shift will be very close to one.

One simple method for partitioning the F different shift positions into M-element groups is to place M adjacent shifts in a

[1]The transmitter can send any pattern of zero and one bits as long as the receiver knows and uses the same pattern. However, since nothing is sent for a zero bit, they are useless during the code acquisition, so only when the transmitter sends a bit one, the check on a cell can be performed.

group, *i.e.,* $\{0, T_c, 2T_c, \ldots, (M-1)T_c\}$ shift positions are selected for the first group and $\{MT_c, (M+1)T_c, \ldots, (2M-1)T_c\}$ for the second and other groups would follow in the same way. For example, in Fig. 6(a) and (b) an OOC with $F = 32$ and $K = 4$ and one possible pattern used for correlation for $M = 3$ are shown.

We consider that the code generator uses "cyclic shift" instead of simple "delayed shift." Consider an OOC code expressed as follows:

$$c(t) = \sum_{i=0}^{F-1} a_i P_{T_c}(t - iT_c) \tag{6}$$

where (a_0, a_1, E, a_{F-1}) is the code pattern. The mth cyclic shift of this code is defined as

$$c_{m,\text{Cyclic-Shift}}(t) = \sum_{i=0}^{F-1} a_{(m+i) \bmod F} P_{T_c}(t - iT_c) \tag{7}$$

while we define the mth delayed shift as

$$\begin{aligned} c_{m,\text{Delayed-Shift}}(t) &= c(t - mT_c) \\ &= \sum_{i=0}^{F-1} a_i P_{T_c}(t - (i+m)T_c). \end{aligned} \tag{8}$$

By using the cyclic shift, it is ensured that the locally generated pattern will at most have a total length of F chips and we can select dwell time to be one bit duration.

Although we consider a simple active correlator structure for examining the shift positions, other receiver structures described in [2]–[4] like matched filter with or without hardlimiter(s) can be also used. It is only required that the structure have the ability to, somehow, compute the decision variable when the first stage examines M shifts simultaneously. For example, if the matched filter structure is used, the decision variable in the first stage can be computed by integrating the output of matched filter in M different chip positions corresponding to the M shifts being examined and then adding the results for these chip positions.

In the multiple-shift algorithm the choice of the parameter M could be of outmost importance, since the arbitrarily increase of this parameter could have two different effects on the performance of the synchronization system. As M increases the number of shifts examined simultaneously increases and, therefore, the search space will be covered in fewer tries. In other words, the parameter Q that represents the number of groups will decrease. On the other hand, with the increase of M, the number of dwell times required to find the correct shift among the M shifts in the second stage will increase. Another effect of increasing M is that the probability of false alarm of the first stage will increase since with the use of a larger value for parameter M, more interference is introduced in the checking process. It is, therefore, expected that an optimum value for M exists for which the performance of the synchronization system is optimum, or equivalently the synchronization time is minimum.

III. Markov Chain Model

To obtain the mathematical derivation of the multiple-shift algorithm, we model it with a Markov state model. It is assumed that the probabilities of false alarm (both in the first and the second stages) are independent of the shift position(s) or cell(s) being examined. Although generally this assumption is not true, for performance analysis we can consider an average probability of false alarm and assign it to every shift position. We denote by P_{FA} and p_{fa} the probabilities of false alarm in the first and the second stages, respectively.

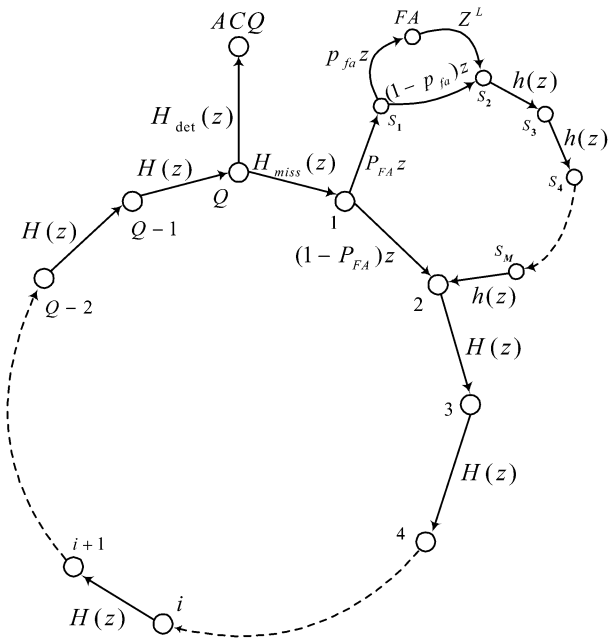

Fig. 2. Markov chain model for multiple-shift algorithm.

Two other probabilities used in the modeling of the algorithm are P_D and p_d which denote respectively the probabilities of detection in the first and the second stages. Probability of detection is simply the probability that we detect the correct shift position and not miss it.

The Markov chain model is illustrated in Fig. 2. It has a main loop consisting of Q different nodes numbered from 1 to Q. Each node in the main loop represents one of the groups in the partition of search space. Since the numbering of the groups is arbitrary, without loss of generality we assume that the correct shift is in the Qth group. The adjacent nodes in the main loop are connected to each other via branches. The exact structure of these branches is shown only between nodes 1 and 2 and for other nodes this structure is represented by an equivalent transfer function, namely, $H(z)$.

From Fig. 2, we observe that each branch have a transfer function representing the probability distribution of transition between the two nodes the branch connects to each other. The power of z in each branch function represents the number of bits (or equivalently dwell times) that is required for this transition. For example the branch connecting node 1 to node 2 with transfer function $(1 - P_{FA})z$, indicates that with probability $(1 - P_{FA})$ we traverse node 1 directly to node 2 and this transition requires only one bit, i.e., all the M shifts in group one are rejected and the algorithm continues to the next step, considering the next group. However, with probability P_{FA} we enter the second stage of the algorithm. The second stage is represented in the Markov chain model by a sub-loop connecting

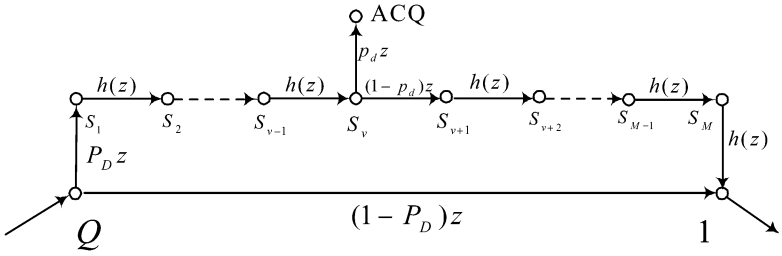

Fig. 3. Branch connecting node Q to node 1.

nodes 1 to 2 consisting of M different nodes $S_1, S_2, \ldots, S_M$. Each of these nodes corresponds to one of the M shifts in the group. The exact branch structure connecting these nodes is shown only between nodes S_1 and S_2 and for other nodes an equivalent function $h(z)$ is used. With probability $(1-p_{fa})$ we directly go to the next node, examining the next shift but with probability p_{fa} we reach the "FA" (false alarm) node. We recover from FA node in L bits time. L is defined to be the number of bits required by the verification mode for detection of false alarm. If we simplify the branches connecting S_1 and S_2 we can represent it with a simple transfer function defined as follows:

$$h(z) = (1-p_{fa})z + p_{fa}z^{L+1}. \tag{9}$$

The whole branch structure connecting node 1 to node 2 can be also simplified into a function $H(z)$ defined as follows:

$$H(z) = (1-P_{FA})z + P_{FA}zh^M(z). \tag{10}$$

The structure is more complicated for the branches connecting node Q to node 1. It is assumed that the correct shift is within the Qth group, i.e., one of the shifts in this group is the correct one. Consider that the group is successfully accepted in the first stage, and assume that the vth shift examined in the second stage among the M shifts of the Qth group is actually the correct shift. Then the structure in Fig. 3 will show the branch connection between node Q and node 1. With probability $(1-P_D)$ we miss the Qth group and go directly to the next group and with probability P_D the second stage is initiated in which all the shifts including the correct shift position (represented by S_v) are examined.

Note that as the selection of groups and the order of elements within a group are both arbitrary, we have no information about the time in the second stage we reach the correct shift. In other words, any of the M shifts in the Qth group can be the correct shift. Thus we assume that v can take any values from the set $\{1, 2, \ldots, M\}$ with equal probability, i.e., we model v as a uniformly distributed random variable.

We can simplify the structure shown in Fig. 3 and model the whole branches with two transfer functions. One connecting node Q to node 1, namely $H_{\text{miss}}(z)$, and the other, $H_{\text{det}}(z)$ between Qth node and ACQ node which is the final node representing the successful end of the search process.

$$H_{\text{det}}^{(v)}(z) = p_d P_D z^2 h^{v-1}(z), \tag{11}$$

$$H_{\text{miss}}^{(v)}(z) = (1-P_D)z + P_D(1-p_d)z^2h^{M-1}(z). \tag{12}$$

Fig. 3 illustrates the branch connections when the vth shift among the M shifts is the correct one, and we modeled v as random variable. The expressions above are therefore both conditioned on v and later after simplifying the entire Markov chain model we will take expectation over this random variable.

Consider that the search begins with the ith group as the first group being examined. In other words we enter the main loop of Markov model shown in Fig. 2 from the ith node. Then the transfer function between input (the ith node) and output (the ACQ node) will be as follows:

$$U_i^{(v)}(z) = \frac{H^{Q-i}(z)H_{\text{det}}^{(v)}(z)}{1 - H_{\text{miss}}^{(v)}(z)H^{Q-1}(z)}. \tag{13}$$

Since the first group to be examined is selected randomly, we assume that we enter the state diagram at any node in the main loop with equal probability. Thus we can model i as a uniform random variable taking values from the set $\{1, \ldots, Q\}$. In this case averaging from (13) over both i and v we obtain

$$U(z) = \frac{H_{\text{det}}(z)}{1 - H_{\text{miss}}(z)H^{Q-1}(z)} \frac{1}{Q} \sum_{i=1}^{Q} H^{Q-i}(z) \tag{14}$$

where $H_{\text{det}}(z)$ and $H_{\text{miss}}(z)$ are defined as follows:

$$\begin{aligned} H_{\text{det}}(z) &= \frac{1}{M}\sum_{v=1}^{N} H_{\text{det}}^{(v)}(z) \\ &= \frac{1}{M} p_d P_D z^2 (1 + h(z) + h^2(z) + \cdots + h^{M-1}(z)) \end{aligned} \tag{15}$$

$$H_{\text{miss}}(z) = (1-P_D)z + P_D(1-p_d)z^2h^{M-1}(z). \tag{16}$$

We denote by N_{Acq} the number of bits (or equivalently the number of dwell times) required by the algorithm to find the correct shift position. N_{Acq} can be modeled as a discrete random variable. It is shown in [7]–[9] that $U(z)$ computed in (14) is the characteristic function (or moment generating function (MGF)) of this random variable defined as follows

$$U(z) = \mathbb{E}(z^{N_{Acq}}). \tag{17}$$

The mean of N_{Acq} can be computed from its MGF as follows:

$$\mathbb{E}(N_{\text{Acq}}) = \left.\frac{dU(z)}{dz}\right|_{z=1} = U'(1). \tag{18}$$

Further, it can be shown that

$$H'(1) = 1 + MP_{FA}(1 + Lp_{fa}) \tag{19}$$

$$\begin{aligned} H'_{\text{det}}(1) &= 2p_dP_D + \frac{M-1}{2}p_dP_D(1 + Lp_{fa}) \\ &= \frac{1}{2}p_dP_D[(M+3) + L(M-1)p_{fa}] \end{aligned} \tag{20}$$

$$\begin{aligned} H'_{\text{miss}} &= (1 - P_D) + P_D(1 - p_d) \\ &\quad \times [M + 1 + (M-1)Lp_{fa}]. \end{aligned} \tag{21}$$

In the Appendix, we prove that after simplifying (14) and (18) we obtain

$$\mathbb{E}(N_{\text{Acq}}) = \frac{H'_{\text{det}}(1) + H'_{\text{miss}}(1)}{p_dP_D} + (Q-1)H'(1)\frac{2 - p_dP_D}{2p_dP_D}. \tag{22}$$

Now consider a special ideal case in which the probabilities of false alarm are both zero and the probabilities of detection are one, i.e., $P_{FA} = p_{fa} = 0$ and $P_D = p_d = 1$. Substituting these values in (14) and (19)–(22) we obtain

$$U(z) = \frac{1}{M}(z + z^2 + \cdots + z^M)\frac{1}{Q}(z + z^2 + \cdots + z^Q) \tag{23}$$

$$\mathbb{E}(N_{\text{Acq}}) = 1 + \frac{M+Q}{2}. \tag{24}$$

From the moment generating function (23) we conclude that N_{Acq} can be modeled as the summation of two independent discrete uniform random variables, one taking values from the set $\{1, 2, \ldots, M\}$ and the other from the set $\{1, 2, \ldots, Q\}$.

Considering the effect of M in (24), we see that with the increase of M the term $M/2$ will increase but $Q(\approx F/M)$ will decrease. Thus there should be an optimum M resulting the minimum $\mathbb{E}(N_{Acq})$. To find the optimum value for M, we consider that M can take on any real value within its range and then we differentiate (24) with respect to M as follows:

$$\frac{\partial \mathbb{E}(N_{\text{Acq}})}{\partial M} = \frac{1}{2} - \frac{F}{2M^2} = 0 \Longrightarrow M_{opt} = \sqrt{F}. \tag{25}$$

Note that M is actually an integer number. Thus, we conclude that optimum M is near square root of F, but it may be the upper closest integer or the lowest closest integer to the square root of F. Substituting this optimum M into (24) we obtain the minimum value for $\mathbb{E}(N_{\text{Acq}})$.

$$\min \mathbb{E}(N_{\text{Acq}}) = 1 + \sqrt{F}. \tag{26}$$

Since we obtained the above result for an ideal case (no false alarm), it can be regarded as a lower bound on the mean number of required bits for the synchronization process. Thus to find the correct shift position, the synchronization system at least requires square root of the number of shifts (F) bits or dwell times. If we compare this result with the result obtained for simple serial-search algorithm [6] which requires about $F/2$ bits, we see the improvement yielded by multiple-shift algorithm, e.g., if $F = 2000$, the simple serial-search requires about 1000 bits even for the ideal case with no false alarm. However, the multiple-shift algorithm's lower bound is only 46 bits.

IV. Probabilities of False Alarm and Detection

In this section, the probabilities of false alarm and detection are computed. We assume that all the delays of different users and even the delay of the locally generated signal are multiples of chip duration T_c, *i.e.,* $\tau_k = \gamma_k T_c$ where $\gamma_k \in \{0, 1, \ldots, F-1\}$ and the locally generated code's chip time matches with the received signal's chips. This condition is called the "chip synchronous" case. This assumption is used for both the desired user's signal and for all the other users' (interfering users) signals. Considering only other users, these assumptions will not only simplify the mathematical structure of the multi-access interference, it further indicates an upper bound on the performance of the system compared to a more realistic chip asynchronous model ([1], [2]). However, for the desired user the chip synchronous assumption is actually the best and not the worst case possible. In fact, the worst case occurs when there is an odd multiple of half chip time difference between the received and the locally generated codes. In this case, even the two codes are matched, the output will be half code weight, i.e., $K/2$. Later in the next section, we discuss more about these assumptions and we show how to resolve the limitation caused by these assumptions.

It can be shown that the probabilities of false alarm and detection not only depend upon the system parameters like the code length (F), the code weight (K), the number of users (N), and the number of shifts in each group (M), but they also depend upon the exact OOC code patterns used in the system. Three different approaches can be employed to compute these probabilities. For the first approach, we use a simulation scheme for computing these probabilities. For the second approach, all the code patterns should be known. Then we can use some specific algorithms to find the probability mass functions (PMF) that are required for determining the performance of the system using these OOC patterns. Unfortunately the result obtained from this method is not a closed form solution and this method is very complicated, unwieldy, and cumbersome.[2] For the third approach, we use some simplifying assumptions that lead to some approximate closed-form expressions for these probabilities. In this section we focus on the third approach.

First let us consider the probability of false alarm in the first stage *i.e.,* P_{FA}. This probability can be expressed as follows:

$$P_{FA} = \mathbb{P}(X \geq TH) \tag{27}$$

where X is the decision variable which is the output of the correlator when M different shifts of desired user's code are multiplied by the received signal. We denote by TH and th the thresholds used, respectively, in the first and the second stages of the algorithm. X can be further modeled as the sum of M variables, each being the output of the correlator due to one of the M shifts. It is shown in [1] that when a single shift of code

[2]As this method requires complicated algorithms and finally the result is not very different from the approximate results obtained in this section we do describe it in this paper.

is considered, the correlator's output will have a binomial distribution expressed as follows:

$$\text{Output due to a single shift} \sim \text{Binomial}\left(N, \frac{K^2}{2F}\right) \quad (28)$$

and X is the sum of M such variables. However, these variables are generally dependent to each other and, therefore, their joint probability mass function is required for computing the PMF of X. As mentioned above computing this joint PMF is very cumbersome and requires complicated algorithms. We use a simplifying assumption, namely, that these M variables are mutually independent. With this assumption, X will be the summation of M independent identically distributed (i.i.d.) random variables each having a binomial distribution. Therefore, it has also a binomial distribution expressed as follows:

$$X \sim \text{Binomial}\left(NM, \frac{K^2}{2F}\right). \quad (29)$$

The following expression is obtained for P_{FA}

$$P_{FA} = \sum_{n=TH}^{NM} \binom{NM}{n} \left(\frac{K^2}{2F}\right)^n \left(1 - \frac{K^2}{2F}\right)^{NM-n}. \quad (30)$$

If we select both the thresholds in the two stages properly, *i.e.,* $K \geq TH$ and $K \geq th$, the probabilities of detection will both be one. For the chip synchronous case, when the correct shift position is examined, we obtain K pulses from the main user and the interference can only increase the number of pulses at the output. Therefore, for the ideal photodetector case we have

$$p_d = P_D = 1 \; (TH \leq K, TH \leq Kth \leq K). \quad (31)$$

If the output of the correlator exceeds the threshold used in the second stage for a wrong shift position, we have a false alarm. However, we reach the second stage when in the first stage false alarm has already been occurred. The p_{fa} can be therefore expressed as a conditional probability as follows:

$$p_{fa} = \mathbb{P}(x \geq th | X \geq TH) \quad (32)$$

where x is defined to be the decision variable in the second stage, i.e., the output of the correlator when a single shift of the desired user's code is correlated with the received signal. Equation (32) can be rewritten as follows:

$$p_{fa} = \frac{\mathbb{P}(x \geq th \cap X \geq TH)}{\mathbb{P}(X \geq TH)}. \quad (33)$$

The denominator of (33) is the same as P_{FA}, which is computed in (30). In order to compute the numerator of (33), we need to define some new variables, namely, $l_1, l_2, \ldots, l_M$. Consider one of the groups in the search space partition for which we want to compute $\mathbb{P}(x \geq th \cap X \geq th)$. We define $l_i (i = 1, 2, \ldots, M)$ to be the number of pulses at the correlator's output when the ith shift of the group is used as the locally generated code and all users are continuously transmitting bit one. Due to the cross-correlation properties of OOCs, each pulse from the l_i pulses at the output of the correlator will be from a different user. Thus l_i further represents the number of users that can interfere with the ith shift of the group. With the assumption that the delays associated with each user have uniform distribution and considering the properties of OOCs, the distribution of each l_i can be obtained. We have N independent interfering users, each can contribute only at most one pulse to the output with probability K^2/F. Thus each l_i have a binomial distribution expressed as follows:

$$l_i \sim \text{Binomial}\left(N, \frac{K^2}{F}\right). \quad (34)$$

Note that we consider the desired user just like any other user in our analysis. In other words, it is assumed that we have N interfering users counting even the desired user, since we may get an interfering pulse from the desired user when the received code and the locally generated code does not match. The probability of getting this pulse is $K(K-1)/F$ instead of K^2/F. However, for obtaining (34) we assume that the probability of getting a pulse from each of the N users is the same. Furthermore, we assume that different l_i s are independent from each other. Although this assumption is not generally true, it is not easy to compute the joint probability mass function of these random variables. And the result obtained with this assumption is very close to the exact result or the result obtained from simulation. We rewrite $\mathbb{P}(x \geq th \cap X \geq th)$ as follows

$$\mathbb{P}(x \geq th \cap X \geq th) = \mathbb{E}\left[\mathbb{P}(x \geq th \cap X \geq th | l_1, \ldots, l_M)\right] \quad (35)$$

where the expectation is taken over all the random variables l_i.

The random variable x only depends on one of the $l_i s$, while X is related to all the M shifts and therefore to all $l_i s (i = 1, 2, \ldots, M)$. We assume that x is related to the first shift among the M shifts. In other words, it is assumed that x is only dependent upon l_1. Note that this assumption does not have any effect on the generality of our result.

Each user can transmit bit one or zero with equal probability in any bit frame. Thus from l_1 users that can interfere with the first shift, each may transmit one or zero independently from other users, i.e., each pulse from the l_1 users may be present or absent with probability 1/2 in any bit frame. Thus, x which represents the number of pulses that are present at the output, conditioned on l_1, has a binomial distribution expressed as follows:

$$(x|l_1) \sim \text{Binomial}\left(l_1, \frac{1}{2}\right). \quad (36)$$

Using the same argument and the assumption that that all $l_1 + l_2 + \cdots + l_M$ pulses are from different users and therefore may be independently on or off with probability 1/2, we obtain

$$(X|l_1, l_2, \ldots, l_M) \sim \text{Binomial}\left(l_1 + \cdots + l_M, \frac{1}{2}\right). \quad (37)$$

The decision variables x and X are computed in two different bit frames. Since $(x|l_1)$ and $(X|l_1, \ldots, l_M)$ are related to the transmitted bits in their bit frame, and bits in different frames

are independent, we conclude that $(x|l_1)$ and $(X|l_1,\ldots,l_M)$ are two independent variables and, therefore, (35) can be simplified as follows:

$$\mathbb{P}(x \geq th \cap X \geq TH) = \mathbb{E}\left[\mathbb{P}(x \geq th|l_1,\ldots,l_M)\mathbb{P}(X \geq TH|l_1,\ldots,l_M)\right]. \quad (38)$$

where from (36) and (37)

$$\mathbb{P}(x \geq th|l_1,\ldots,l_M) = \sum_{x=th}^{l_1} \binom{l_1}{x} \left(\frac{1}{2}\right)^{l_1} \quad (39)$$

$$\mathbb{P}(X \geq TH|l_1,\ldots,l_M) = \sum_{X=TH}^{l_1+\cdots+l_M} \binom{l_1+\cdots+l_M}{X} \times \left(\frac{1}{2}\right)^{l_1+\cdots+l_M}. \quad (40)$$

Combining (34), (38)–(40), and simplifying the result, we obtain

$$\mathbb{P}(x \geq th \cap X \geq TH) = \sum_{l_1=0}^{N} \sum_{l=0}^{N(M-1)} \left\{ \binom{N}{l_1} \left(\frac{K^2}{F}\right)^{l_1} \left(1-\frac{K^2}{F}\right)^{N-l_1} \times \binom{N(M-1)}{l} \left(\frac{K^2}{F}\right)^{l} \left(1-\frac{K^2}{F}\right)^{N(M-1)-l} \times \sum_{x=th}^{l_1} \binom{l_1}{x} \left(\frac{1}{2}\right)^{l_1} \sum_{X=TH}^{l_1+l} \binom{l_1+l}{X} \left(\frac{1}{2}\right)^{l_1+l} \right\}. \quad (41)$$

V. Numerical Results

As mentioned in Section IV, we have used some approximations and assumptions to obtain the probabilities of false alarm and detection. Here, in this section we show that the approximate expressions obtained in Section IV, are close to the exact performance of the system. In Fig. 4 we see $\mathbb{E}(N_{\rm Acq})$ versus M for different number of users, N. The solid curves are the results obtained from the expressions of the pervious section. Moreover, some other curves, which are obtained from simulating the synchronization system, are also shown in this figure. The simulation is done in two methods. For the first method, a specific set of OOCs is selected and the mean number of required bits for acquisition is obtained by simulating the system and the multiple-shift algorithm. The dash–dotted curves of Fig. 4 for $N = 5$ are some examples of the results obtained by this method. An important point we draw from the simulation results is that the performance of the synchronization system or more specifically the probabilities of false alarm depend upon the exact form of OOCs used in the system. For the second method, the multiple-shift algorithm is again simulated for many times, but each time a new set of OOCs is generated and used in a random fashion. The dotted curves of Fig. 4 are obtained in this way. This method therefore not only takes an average over the multiaccess interference but it also takes an average over all the possible OOC code patterns that can be used in the system. From Fig. 4 we observe that the curves obtained by this method are very close to the curves obtained from the approximate expressions.

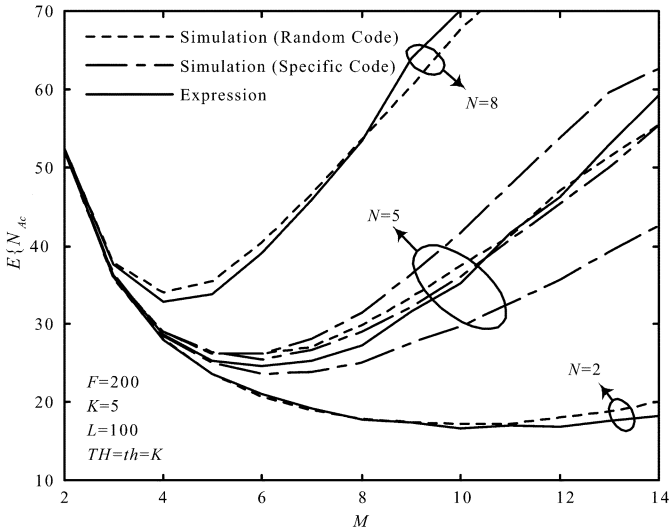

Fig. 4. Comparison of the expressions with simulation results. $E\{N_{Acq}\}$ versus M for a system with parameters $F = 200$, $K = 5$, $L = 100$, $TH = th = K$.

Fig. 5 shows the mean number of required bits $(\mathbb{E}(N_{\rm Acq}))$ for different values of parameters M and N. As expected, for each value of N we can find an optimum value for M. The solid line in Fig. 5(a) shows this optimum value of M. As the number of users increases, the optimum M will decrease and the sensitivity of the performance with respect to the parameter M will also increase, *i.e.,* variation in the parameter M has more effect on the mean number of required bits for larger values of N. For example when $N = 5$ the parameter M can be selected between 20 to 35 in order for the mean number of bits to remain close to its minimum, but the same range for $N = 25$ is between 6 to 9. The dash-dotted line in Fig. 5(b) corresponds to the lower bound obtained in Section III. We observe that for small values of N we can reach this lower bound.

In the previous section, we described our chip synchronous assumptions. Although these assumptions correspond to the worst case for the multi-access interference signal, they are the best possible case for the desired user's signal. However, to ensure that the results obtained are upper bounds on the performance of the system we need to consider the worst case in our analysis for the desired user's signal as well. This worst case occurs when there is a half chip time difference between the desired and the locally generated codes. For this worst case when the two codes are matched, the output of the correlator will be $K/2$ (half code weight) pulses instead of K pulses.

The easy and readily available solution of this problem is to select both the thresholds in the first and the second stages of the algorithm to be below $K/2$. However, the performance of the synchronization system degrades severely with lowering the thresholds, especially the threshold used in the first stage (TH). It is therefore desirable to select the threshold in the first stage as large as possible. If the search space is divided in a way that the shifts in each group are adjacent to each other just as described in Section II, this problem can be solved with a simple modification of the locally generated code pattern. We simply add two pulses with half chip-time duration at the beginning and

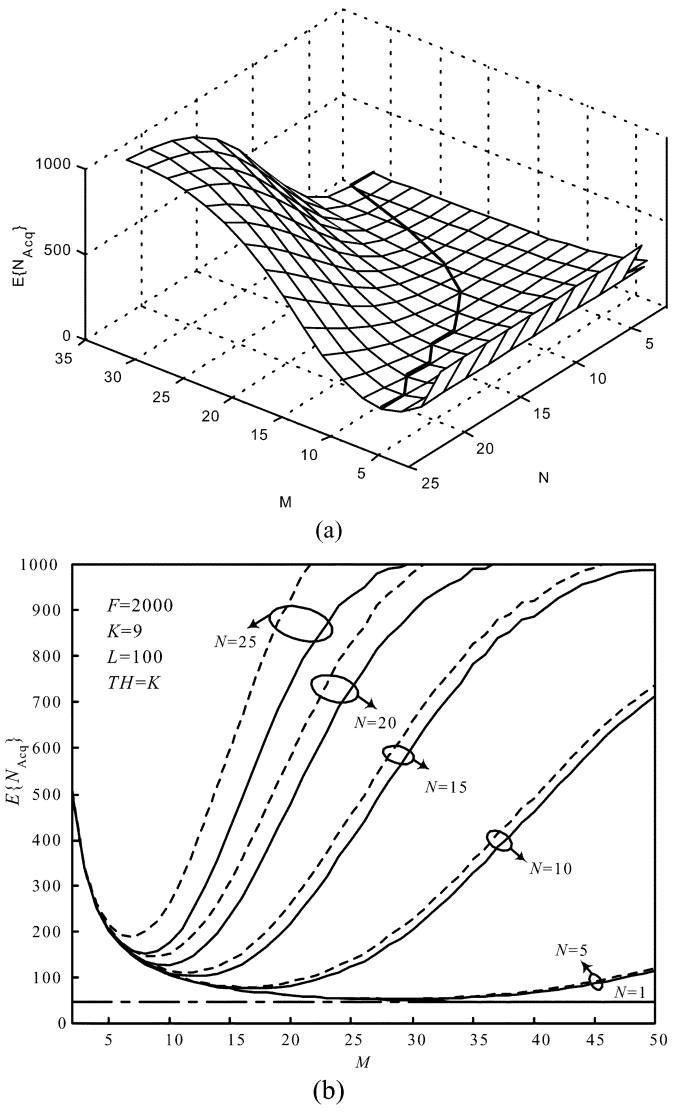

Fig. 5. Effect of M and N for a system with parameters $F = 2000$, $K = 9$, $L = 100$ (a) the solid line represents the optimum M, (b) the solid curves represent the ordinary case ($TH = th = K$), and the dotted curves represent the modified code pattern case, ($TH = K, th = K/2$).

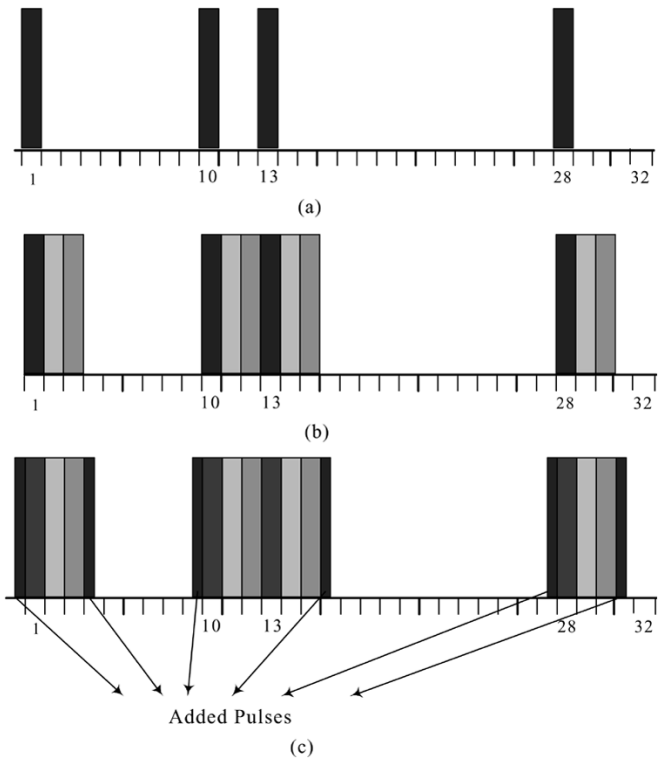

Fig. 6. (a) An OOC with $F = 32$ and $K = 4$. (b) One possible pattern for $M = 3$. (c) The modified pattern.

the end of each large pulse in the pattern. Fig. 6 illustrates how this task is done. Stated another way, we simply add another shift to the pattern, or equivalently increase M by one. With this modification, when the received code does not completely match with one of the shifts, it will coincide with its adjacent shifts and therefore all the K pulses will be seen. The added small pulses guarantee that the output will consist of all the K pulses when the received signal is matched with the first or last shift among the M shifts in the group. This modification can be simply used with other receiver structures. For example, for the matched filter (passive correlator) receiver structure, we extend the duration of integration of the output of matched filter from M chips to $M + 1$ chip positions. With this modification the amount of interference in the decision variable will slightly increase since the number of shifts examined simultaneously has increased from M to $M+1$, but this change enable us to select K as the threshold in first stage and be sure that the correct shift position will not be missed. In Fig. 5(b) the dotted curves represent the result obtained with this modification, i.e., for computing P_{FA} we used $M + 1$ instead of M and $K/2$ is selected as the threshold in the second stage. We observe that for small values of N the two curves, namely the solid curves representing the ordinary case with both thresholds equal K and the dotted curves representing this modified case, are very close to each other, but for larger values of N the difference between them is increased. However, the value of M for which each curve is minimum, namely optimum M, is nearly the same for both the two curves.

Fig. 7 illustrates the effect of N and L on the synchronization system's performance. Fig. 7(a) shows optimum M versus N for three different values of L. The optimum mean number of required bits, i.e., $\mathbb{E}(N_{\rm Acq})$, obtained for the optimum value of M is shown in Fig. 7(b) versus N. We observe that as N increases, the optimum value for M will decrease and consequently the optimum mean number of bits will increase.

The optimum M and $\mathbb{E}(N_{\rm Acq})$ resulting from this optimum M are plotted with respect to code weight, i.e., K, in Fig. 8. We observe that with the increase of K the optimum M will decrease. Since with fixed number of users the increase of K is equivalent to sending more pulses into the channel and, therefore, increasing the multiaccess interference which consequently leads to a smaller value for optimum M. Furthermore, from Fig. 8 we observe that for each value of N, there exists an optimum value for code weight K, for which the mean number of required bits is minimum, e.g., $K = 4$ leads to the minimum $\mathbb{E}(N_{Acq})$ for $N = 15$.

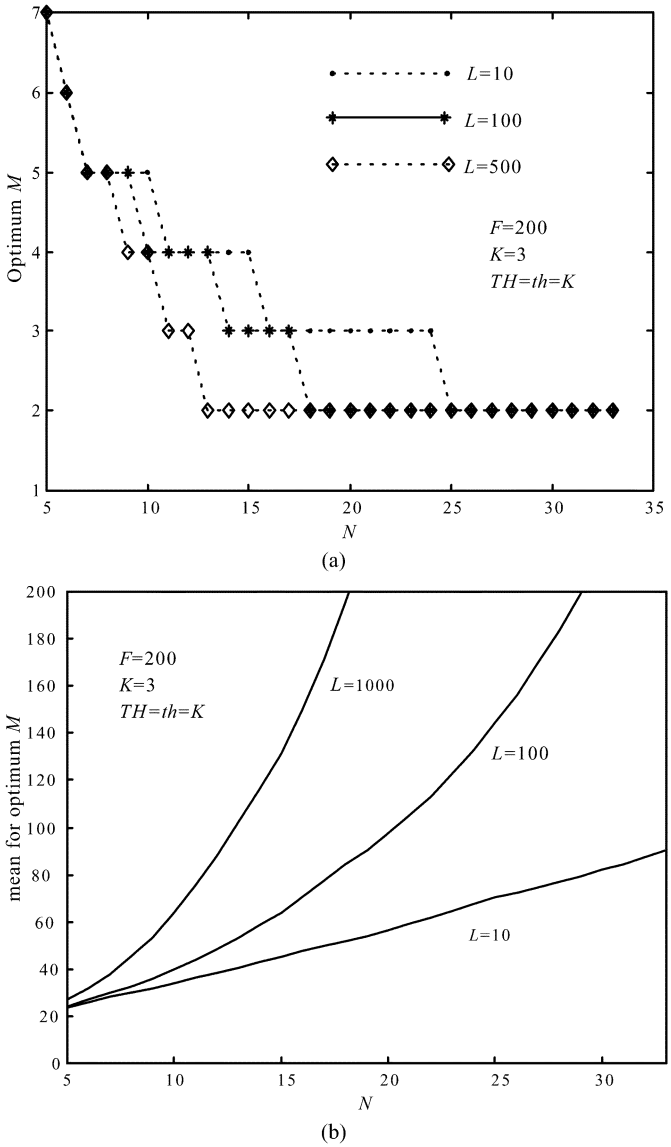

Fig. 7. Effect of N and L on the performance of the synchronization system with parameters $F = 200$, $K = 3$, and $TH = th = K$. (a) Optimum M versus N for different values of L. (b) Optimum $E\{N_{\rm Acq}\}$ versus N for different values of L.

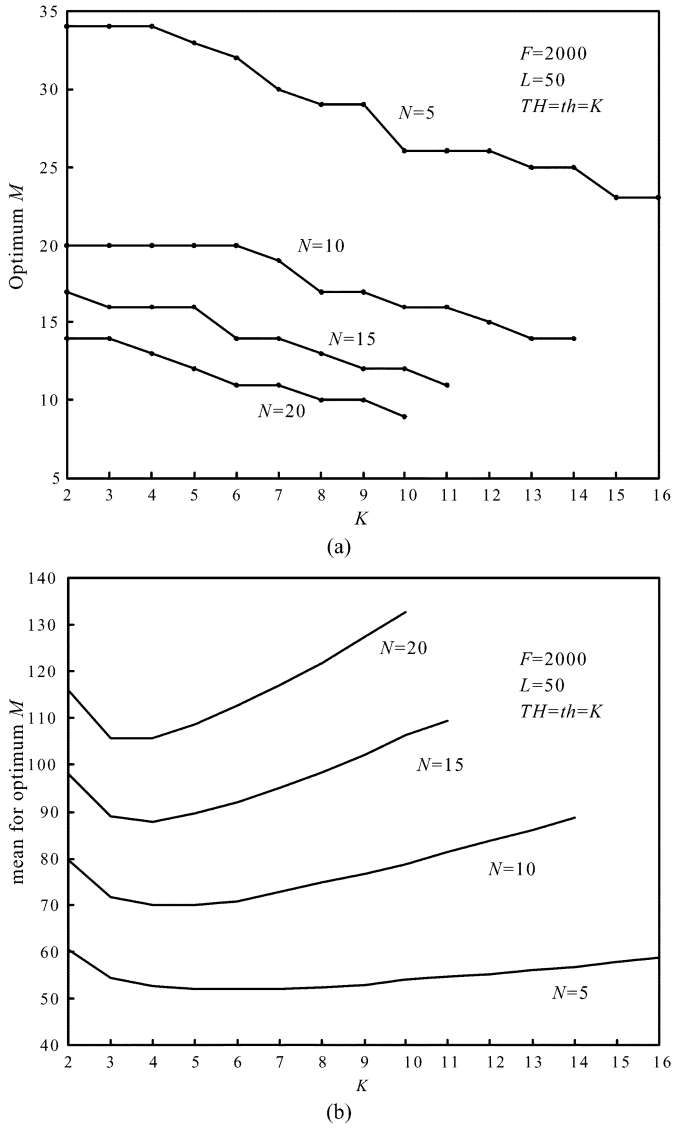

Fig. 8. Effect of code weight on the performance of the synchronization system with parameters $F = 2000, L = 50$ and $TH = th = K$. (a) Optimum M versus K, for different values of N. (b) Optimum $E\{N_{\rm Acq}\}$ versus K for different values of N.

VI. Conclusion

In this paper, we introduced multiple-shift algorithm for code acquisition of OOC codes in an optical CDMA system. We described the algorithm and analyzed its performance regardless of the structure of the receiver with the help of Markov chain model. Then we obtained a general bound on the performance of algorithm. Although the algorithm has the capability to be used with different receiver structures, we only considered the active correlator structure with ideal photodetection for further analysis. However, the consideration of shot noise or other noise sources and other receiver structures is straightforward. With many figures, we illustrated the effect of number of users, code weight and other system parameters on the performance of the synchronization system.

The multiple-shift algorithm is actually an efficient serial-search method that can be regarded as a variation of binary search method and therefore can be used in many other applications other than code acquisition. For example, it can be used in time synchronization, *i.e.,* finding the correct sampling time in a typical communication system, or equivalently finding the peak of a noisy signal.

Appendix

In this appendix, we explain the details of obtaining (22) from (14) and (18). Note that from (9), (10), (15), and (16) we obtain $h(1) = H(1) = U(1) = 1$ and $H_{\rm det}(1) = 1 - H_{\rm miss}(1) = p_d P_D$. We rewrite expression (14) in the form $U(z) = V(z)W(z)$ where $V(z)$ and $W(z)$ are defined as follows:

$$V(z) = \frac{H_{\rm det}(z)}{1 - H_{\rm miss}(z)H^{Q-1}(z)} \tag{42}$$

$$W(z) = \frac{1}{Q}\sum_{i=1}^{Q} H^{Q-i}(z). \tag{43}$$

$$V'(1) = \frac{H'_{\rm det}(1)\left[1 - H_{\rm miss}(1)\right] + \left[H'_{\rm miss}(1) + (Q-1)H_{\rm miss}(1)H'(1)\right] H_{\rm det}(1)}{H^2_{\rm det}(1)}$$
$$= \frac{H'_{\rm det}(1) + H'_{\rm miss}(1)}{p_d P_D} + (Q-1)H'(1)\frac{1 - p_d P_D}{p_d P_D}. \quad (44)$$

$$W'(1) = \frac{1}{Q}\left[1 + 2 + \cdots + (Q-1)\right] H'(1) = \frac{Q-1}{2} H'(1) \quad (45)$$

Note that $V(1) = W(1) = 1$. Therefore $U'(1) = V'(1) + W'(1)$, as shown in (44) and (45) at the top of the page.

Combining (44) and (45), we obtain (22).

ACKNOWLEDGMENT

The authors would like to thank Dr. M. Nasiri-Kenari, M. Razavi, and S. Zahedi for many fruitful discussions. They also thank Dr. M. Hakkak and Dr. M. Beik-Zadeh for support of this research.

REFERENCES

[1] J. A. Salehi, "Code division multiple-access techniques in optical fiber networks—Part I: Fundamental principles," *IEEE Trans. Commun.*, vol. 37, no. 8, pp. 824–833, Aug. 1989.

[2] J. A. Salehi and C. A. Brackett, "Code division multiple-access techniques in optical fiber networks—Part II: System performance analysis," *IEEE Trans. Commun.*, vol. 37, no. 8, pp. 834–842, Aug. 1989.

[3] M. Azizoglu, J. A. Salehi, and Y. Li, "Optical CDMA via temporal codes," *IEEE Trans. Commun.*, vol. 40, no. 7, pp. 1162–1170, Jul. 1992.

[4] S. Zahedi and J. A. Salehi, "Analytical comparison of various fiber-optic CDMA receiver structure," *J. Lightw. Technol.*, vol. 18, no. 12, pp. 1718–1727, Dec. 2000.

[5] M. Razavi and J. A. Salehi, "Fiber optic CDMA networks incorporating multiple optical amplifier," in *Proc. IEEE Globecom Conf.*, vol. II, Nov.–Dec. 2000, pp. 1247–1253.

[6] A. Keshavarzian and J. A. Salehi, "Optical orthogonal code acquisition in fiber-optic CDMA systems via the simple serial-search method," *IEEE Trans. Commun.*, vol. 50, no. 3, pp. 473–483, Mar. 2002.

[7] A. Polydoros, "On the synchronization aspect of direct-sequence spread spectrum systems," Ph.D. dissertation, Dep. Elect. Eng., Univ. of Southern California, Los Angeles, 1982.

[8] A. Polydoros and C. L. Weber, "A unified approach to serial-search spread spectrum code acquisition—Part I: General theory," *IEEE Trans. Commun.*, vol. COM-32, no. 5, pp. 542–549, May 1984.

[9] M. K. Simon, J. K. Omura, R. A. Scholtz, and B. K. Levitt, *Spread Spectrum Communications*. New York: Computer Science Press, 1985, vol. 3.

[10] G. C. Yang, "Performance analysis for synchronization and system on CDMA optical fiber networks," *IEICE Trans. Comm.*, vol. E77B, no. 10, pp. 1238–1248, Oct. 1994.

[11] M. M. Mustapha and R. F. Ormondroyd, "Performance of a serial-search synchronizer for fiber-based optical CDMA systems in the presence of multi-user interference," in *Proc. SPIE*, vol. 3899, Nov. 1999, pp. 297–306.

[12] ——, "Dual-threshold sequential detection code synchronization for an optical CDMA network in presence of multi-user interference," *J. Lightw. Technol.*, vol. 18, no. 12, pp. 1742–1748, Dec. 2000.

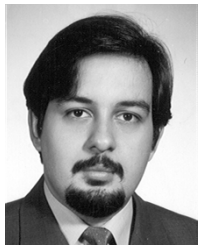

Abtin Keshavarzian (S'99) was born in 1977. He received the B.S. and M.S. degrees (with honors) in Electrical Engineering from Sharif University of Technology, Tehran, Iran, in 1999 and 2001, respectively. He is currently working toward the Ph.D. degree in the Information Systems Laboratory, Electrical Engineering Department, Stanford University, Stanford, CA. His research interests include optical communications systems, wireless sensor networks, and packet switching.

Jawad A. Salehi (S'80–M'84) was born in Kazemain, Iraq, on December 22, 1956. He received the B.S. degree in electrical engineering from the University of California, Irvine, in 1979, and the M.S. and Ph.D. degrees from the University of Southern California (USC), Los Angeles, in 1980 and 1984, respectively.

From 1981 to 1984, he was a full-time Research Assistant at the Communication Science Institute at USC, engaged in research in the area of spread spectrum systems. From 1984 to 1993, he was a Member of Technical Staff with the Applied Research Area at Bell Communications Research (Bellcore), Morristown, NJ. From February to May 1990, he was with the Laboratory of Information and Decision Systems at the Massachusetts Institute of Technology (MIT), Cambridge, as a Visiting Research Scientist conducting research on optical multiple-access networks. From 1997 to 2003, he was an associated professor, and is currently a Full Professor with the Electrical Engineering Department at Sharif University of Technology (SUT), Tehran, Iran. From fall 1999 till fall 2001 he was the head of Mobile Communications Systems group and Co-Director of Advanced and Wideband CDMA Lab at Iran Telecom Research Center (ITRC) conducting research in the area of advance CDMA techniques for optical and radio communications systems. Since 2003, he has funded and directed Optical Network Research Laboratory, at the Electrical Engineering Department of SUT, where advanced experimental and theoretical research on futuristic optical networks are conducted. His current research interests are in the areas of optical multi-access networks, in particular, optical orthogonal codes (OOCs), fiber-optic CDMA, femtosecond or ultra-short light pulse CDMA, spread time CDMA, holographic CDMA, wireless indoor infrared CDMA, all-optical synchronization, and applications of EDFA in optical systems. His work on optical CDMA resulted in 11 U.S. patents.

Dr. Salehi is a recipient of the Bellcore's Award of Excellence. He has also received the Outstanding Research Award of the Electrical Engineering Department at SUT, Tehran, Iran, in 2002, the Outstanding Research Award of the Electrical Engineering Department at SUT, Tehran, Iran, in 2003, the Outstanding Research Award of SUT, Tehran, Iran, in 2003, the Nationwide Outstanding Research Award from the Ministry of Higher Education, in 2003, and the Special Nationwide Outstanding Research Award in 2004. Recently, he was introduced as being among the 250 prominent and most influential researchers worldwide by ISI Highly cited in the computer science category. He is the co-recipient of IEEE's Best Paper Award from the International Symposium on Communications and Information Technology, Japan, October 2004. He assisted, as a member of the organizing committee, in organizing the first and the second IEEE Conference on Neural Information. Since May 2001, he has been serving as Editor for Optical CDMA of the IEEE TRANSACTIONS ON COMMUNICATIONS.